Cell Host & Microbe
Article

Dengue Virus-Induced Autophagy Regulates Lipid Metabolism

Nicholas S. Heaton[1] and Glenn Randall[1,*]
[1]Department of Microbiology, The University of Chicago, Chicago, IL 60637, USA
*Correspondence: grandall@bsd.uchicago.edu
DOI 10.1016/j.chom.2010.10.006

SUMMARY

Autophagy influences numerous cellular processes, including innate and adaptive immunity against intracellular pathogens. However, some viruses, including dengue virus (DENV), usurp autophagy to enhance their replication. The mechanism for a positive role of autophagy in DENV infection is unclear. We present data that DENV induction of autophagy regulates cellular lipid metabolism. DENV infection leads to an autophagy-dependent processing of lipid droplets and triglycerides to release free fatty acids. This results in an increase in cellular β-oxidation, which generates ATP. These processes are required for efficient DENV replication. Importantly, exogenous fatty acids can supplant the requirement of autophagy in DENV replication. These results define a role for autophagy in DENV infection and provide a mechanism by which viruses can alter cellular lipid metabolism to promote their replication.

INTRODUCTION

Autophagy is a cellular process by which cytoplasmic components are sequestered in double-membrane vesicles and degraded to maintain cellular homeostasis (Mizushima, 2007). It has also been implicated as an important component of the innate and adaptive immune response against a variety of viral and bacterial pathogens (reviewed in Deretic, 2005; Deretic and Levine, 2009; Kirkegaard et al., 2004; Schmid et al., 2006). Intact autophagocytic machinery has been reported to contribute to defense against infection by herpes simplex virus-1 (Orvedahl et al., 2007), vesicular stomatitis virus (Shelly et al., 2009), and Sindbis virus (Liang et al., 1998).

Some viruses, however, require components of the autophagocytic machinery for robust replication (reviewed in Deretic and Levine, 2009). In particular, many positive-stranded RNA viruses require autophagy for efficient replication. Members of the family Picornaviridae, such as poliovirus (Jackson et al., 2005; Taylor and Kirkegaard, 2007) and coxsackieviruses B3 (Wong et al., 2008) and B4 (Yoon et al., 2008), have reduced replication in the presence of autophagy inhibitors. Further, markers of poliovirus replication and autophagosomes colocalize in infected cells, which has led to the hypothesis that polio virus replication structures may be at least in part derived from autophagosomes (Jackson et al., 2005). In addition to the Picornaviridae, members of the Flaviviridae, hepatitis C virus (HCV) (Dreux et al., 2009; Sir et al., 2008), and dengue virus (DENV) have been shown to require autophagy (or a component of autophagic machinery) for efficient replication. Several reports have shown that DENV infection induces autophagy and that the inhibition of autophagy leads to a significant reduction in DENV replication and the release of viral particles (Heaton et al., 2010; Khakpoor et al., 2009; Lee et al., 2008; Panyasrivanit et al., 2009).

After virion endocytosis and uncoating, DENV proteins are translated and establish membranous replication complexes in the cytosol that facilitate efficient viral RNA replication (Miller and Krijnse-Locker, 2008). A proteolytically processed form of DENV NS4A protein, termed NS4A-2K, appears to be sufficient for DENV membrane remodeling, perhaps performing a structural role by inducing membrane curvature (Miller et al., 2007). It was previously postulated that DENV-2 replicates on amphisomes, which are fused endosomes and autophagosomes (Khakpoor et al., 2009; Panyasrivanit et al., 2009). However, this hypothesis is inconsistent with the cryo-electron microscopy (cryo-EM) tomography data, which show that viral RNA replication complexes are contiguous with the endoplasmic reticulum (ER) and thus are not distinct structures (Welsch et al., 2009). Therefore, although several groups have characterized autophagy as an important determinant for DENV replication, the role of autophagy in DENV infection is unclear.

Recently, autophagy has been show to regulate cellular lipid metabolism by modifying lipid droplets (Singh et al., 2009), which are cellular stores of triglycerides (TGs) and cholesterol esters (Martin and Parton, 2006). The TGs are processed by lipases, which results in the release of fatty acids (Haemmerle et al., 2003), which are then imported via the carnitine carrier system into mitochondria (McGarry and Brown, 1997), where they undergo β-oxidation (Ren and Schulz, 2003) that eventually leads to ATP production (Jormakka et al., 2003). The role of autophagy in maintaining normal cellular physiology is well established; yeast deficient in autophagy rapidly die under low-nutrient conditions (Tsukada and Ohsumi, 1993) and mice with impaired autophagy have abnormal cellular membrane inclusions and protein aggregates (Komatsu et al., 2005). In addition, many human diseases are associated with deregulated autophagosome formation, including neurodegenerative diseases, myopathies, and liver injury (Mizushima et al., 2002; Perlmutter, 2002).

In this study, we investigated whether DENV-induced autophagy regulates lipid metabolism. We found that the induction of autophagy in DENV-infected cells correlates with decreases in lipid droplet area and triglyceride levels and increases in β-oxidation. These alterations in lipid metabolism are autophagy dependent and are required for efficient DENV replication.

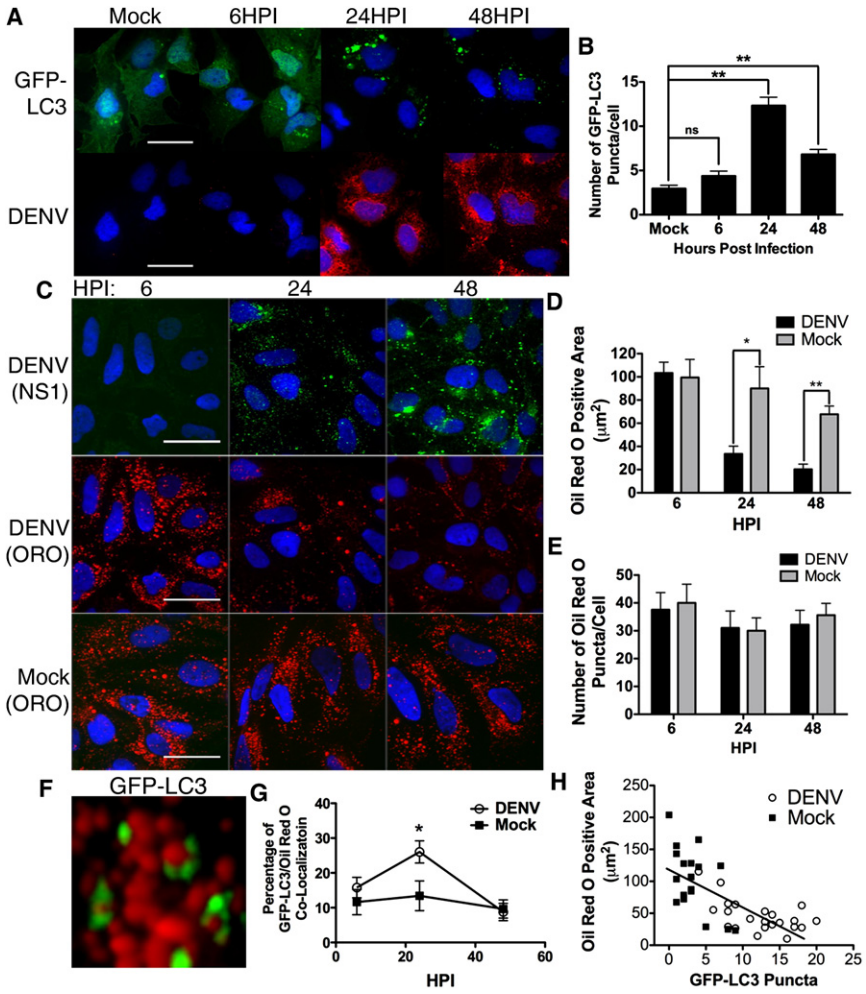

Figure 1. Lipid Droplet Area Decreases as the Number of GFP-LC3 Puncta Increase in DENV-Infected Cells

(A) Huh-7.5 cells were transfected with a GFP-LC3 construct and then DENV- or mock-infected at an moi of 2 for the indicated times, fixed, and probed with specific monoclonal antibody D1-4G2-4-15. Nuclei were visualized by DAPI staining. The scale bar represents 30 μm.

(B) ImageJ quantification of the number of GFP-LC3 puncta per cell in (A). **$p < 0.001$.

(C) Huh-7.5 cells were DENV- or mock-infected at an moi of 2 for the indicated times and then stained with oil red O to visualize lipid droplets, and antibodies to NS1 were used to verify cells were infected. The scale bar represents 30 μm.

(D) Quantification of the total oil red O-positive area per cell representative of three independent experiments. *$p < 0.05$, **$p < 0.001$.

(E) Quantification of the number of oil red O puncta per cell.

(F) Huh-7.5 cells were transfected with a GFP-LC3 construct, DENV-infected for 36 hr, and stained with oil red O. A high-magnification image of GFP-LC3 association with lipid droplets is shown.

(G) Huh7.5 cells were DENV- or mock-infected for the indicated times. The association of GFP-LC3-positive structures with oil red O is quantified, *$p < 0.05$.

(H) Scatter plot of the number of lipid droplets and GFP-LC3 puncta in individual DENV- or mock-infected cells from random fields of view, 36 HPI. The trend line indicates a statistically significant ($p < 0.05$) linear regression showing a negative correlation between the two variables. Error bars represent the standard error of the mean (SEM).

Complementation studies demonstrated that although autophagy regulates many cellular processes, its modulation of lipid metabolism is the requirement for efficient DENV replication.

RESULTS

Induction and Localization of Autophagosomes in DENV-Infected Cells

We first examined the subcellular localization of autophagosomes in DENV-infected cells. In order to visualize autophagosomes, we fused GFP to LC3, which specifically associates with autophagosomal membranes. Huh-7.5 cells were transfected with GFP-LC3 for 24 hr; infected with DENV for 6, 24, or 48 hr; and fixed, probed with DENV2-specific monoclonal antibody D1-4G2-4-15, and visualized with confocal microscopy. Consistent with previous reports, the number of GFP-LC3 puncta per DENV-infected cell significantly increased at 24 and 48 hr postinfection (HPI), compared with mock-infected cells ($p < 0.001$, Figures 1A and 1B).

We then investigated whether GFP-LC3 colocalizes with markers of DENV replication complexes by using antibodies that recognize NS1, NS3, or dsRNA, the positive-strand RNA virus replication intermediate. We were unable to identify conditions in which GFP-LC3-positive structures colocalized with markers of DENV replication (Figure S1, available online). In some cases, the GFP-LC3 localization was reminiscent of lipid droplet distributions in Huh-7.5 cells. Therefore, we examined colocalization of GFP-LC3 with lipid droplets in DENV-infected cells. Huh-7.5 cells were transfected with GFP-LC3, infected with DENV for 24 hr, fixed, and stained with oil red O. We observed a subset of GFP-LC3-positive autophagosomes associating with lipid droplets in DENV-infected cells (Figures 1F and 5D). A kinetic analysis of autophagosome association with lipid droplets showed maximal association 24 hr after DENV infection (Figure 1G).

DENV-Induced Autophagy Reduces Cellular Lipid Droplet Area

We next examined whether lipid droplets were modified in DENV-infected cells. Huh-7.5 cells were infected as before, fixed, probed with antibody to NS1, and stained with oil red O. Lipid droplet area was reduced by ~70% in DENV-infected cells at 48 HPI, compared with mock-infected cells ($p < 0.001$, Figures 1C and 1D). Despite this decrease in total oil red O staining area

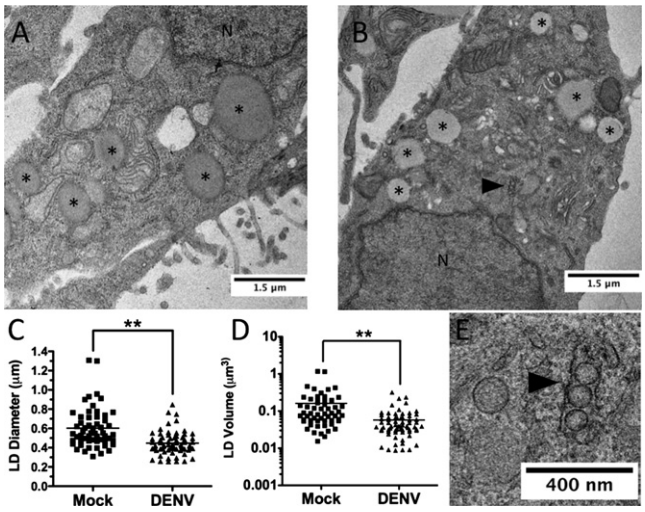

Figure 2. EM Analysis of Lipid Droplet Size during DENV Infection

Huh-7.5 cells were DENV- or mock-infected (moi = 2) for 48 hr, fixed, and pelleted for EM staining and sectioning. Representative images of (A) mock- and (B) DENV-infected cells are shown. * denotes lipid droplets, N denotes the nucleus, and the black arrowhead in (B) denotes DENV-induced membrane structures. Plots of the (C) average diameter and (D) calculated volume of lipid droplets (n > 50) in EM images are shown. **p < 0.001. (E) High-magnification image of (B) shows DENV-induced membrane reorganization.

per cell, the total number of oil red O foci per cell remained relatively unchanged (Figure 1E). This indicated that lipid droplets were not eliminated in DENV infection but that their size, and possibly content, was reduced. The results were reproduced in BHK, Huh7, and HepG2 cells to confirm that effects were not cell type specific (Figure S2).

Lipid droplets were generally depleted in cells with high numbers of autophagosomes. To test for a direct correlation, we quantified the number of autophagosomes and lipid droplet area per mock- and DENV-infected cells and performed a linear regression analysis. There was a statistically significant ($p < 0.05$) negative correlation between the number of autophagosomes and the area of lipid droplets per cell (Figure 1H).

Because oil red O staining is an indirect measurement of lipid droplet area, we next quantified the size of lipid droplets in DENV-infected and mock-infected cells after visualization by EM (Figures 2A and 2B). Huh-7.5 cells were mock- or DENV-infected for 48 hr and then fixed and processed for EM. The lipid droplet diameters in these cells were then measured. DENV infection was verified by the presence of virally induced membrane structures (Figures 2B and 2E). Lipid droplet diameter in DENV-infected cells was decreased ~35% compared to mock-infected cells, which translated to an ~70% reduction in lipid droplet volume ($p < 0.001$, Figures 2C and 2D).

Autophagy Is Required for Lipid Droplet Depletion during DENV infection

We next tested whether autophagy was required for the alterations of lipid droplets in DENV-infected cells. Huh-7.5 cells were infected as before and treated with 3-methyladenine (3MA), a well-characterized inhibitor of autophagy. In addition, we inhibited autophagy by silencing key components of the autophagy pathway (ATG12 and BECN1) compared to an irrelevant siRNA (IRR) that targets HCV. In IRR- or vehicle-treated cells, lipid droplet area was again depleted in DENV-infected cells compared to mock-infected cells ($p < 0.001$, Figures 3A and 3B), with only minor changes to lipid droplet number (Figure 3C). Inhibition of autophagy significantly increased the area of lipid droplets in DENV-infected cells (Figures 3D–3F). In parallel, we confirmed that the siRNAs specifically reduced accumulation of the target gene mRNAs (Table S1) and protein (Figure S3A) and that treatment with 3MA or siRNAs targeting autophagy genes precluded the induction of GFP-LC3 puncta during DENV infection (Figure S3B).

Inhibition of Autophagy Leads to a Defect in Viral RNA Replication

We next investigated the stage of the viral life cycle that requires autophagy. To determine whether autophagy plays a role in viral entry, we transfected IRR or BECN1 siRNAs into Huh-7.5 cells and then infected the cells (moi = 0.5) for 15 hr and fixed and stained them for dsRNA as a marker of viral infection (Figures 4A and 4B). Approximately 60% of cells (11 random fields of view, n > 100 cells) in both treatments stained positive for dsRNA, indicating that under the conditions tested, autophagy has no apparent role in viral entry.

It has been reported that autophagy plays a role in translation of HCV RNA (Dreux et al., 2009). To determine whether this was the case during DENV infection, we introduced a DENV-luciferase-reporter-replicon construct with a polymerase mutation (GDD→GΔΔ) and measured luciferase over time. In cells either silenced for BECN1 or treated with 3MA, there was no significant reduction in RNA translation compared to their respective controls (Figures 4C and 4E). In parallel, we introduced the wild-type replicon and again observed no defect in the early translation peak but significant inhibition of replication at later time points ($p < 0.05$, Figures 4D and 4F). The decreases in DENV replication under conditions of inhibited autophagy are also reflected in infectious DENV production. Treatment of Huh-7.5 cells with 3MA or siRNAs targeting BECN1 inhibits infectious DENV production, as has been reported previously (Figures 4G and 4H) (Khakpoor et al., 2009; Lee et al., 2008; Panyasrivanit et al., 2009). 3MA inhibition of DENV replication and infectious virus production is consistent in all cell lines tested, including Huh-7.5, Huh7, HepG2, and BHK cells (Figure S4). We therefore conclude that autophagy is primarily required for DENV replication, although a secondary role in assembly or egress cannot be excluded.

Lipid Delivery to the Lysosomal Compartment Is Increased during DENV Infection

We next characterized autophagosomal maturation during DENV infection. Huh-7.5 cells were DENV- or mock-infected for 24 hr and fixed and analyzed for GFP-LC3 association with the late endosomal and lysosomal marker LAMP1. The majority of GFP-LC3-positive structures are copositive for LAMP1. (Figures 5A and 5B). Autophagosomal acidification was investigated under the same conditions by examining GFP-LC3 colocalization with Lysotracker Red, a fluorescent probe that selectively accumulates in low pH compartments. In mock- and DENV-infected cells, we observed that the majority of

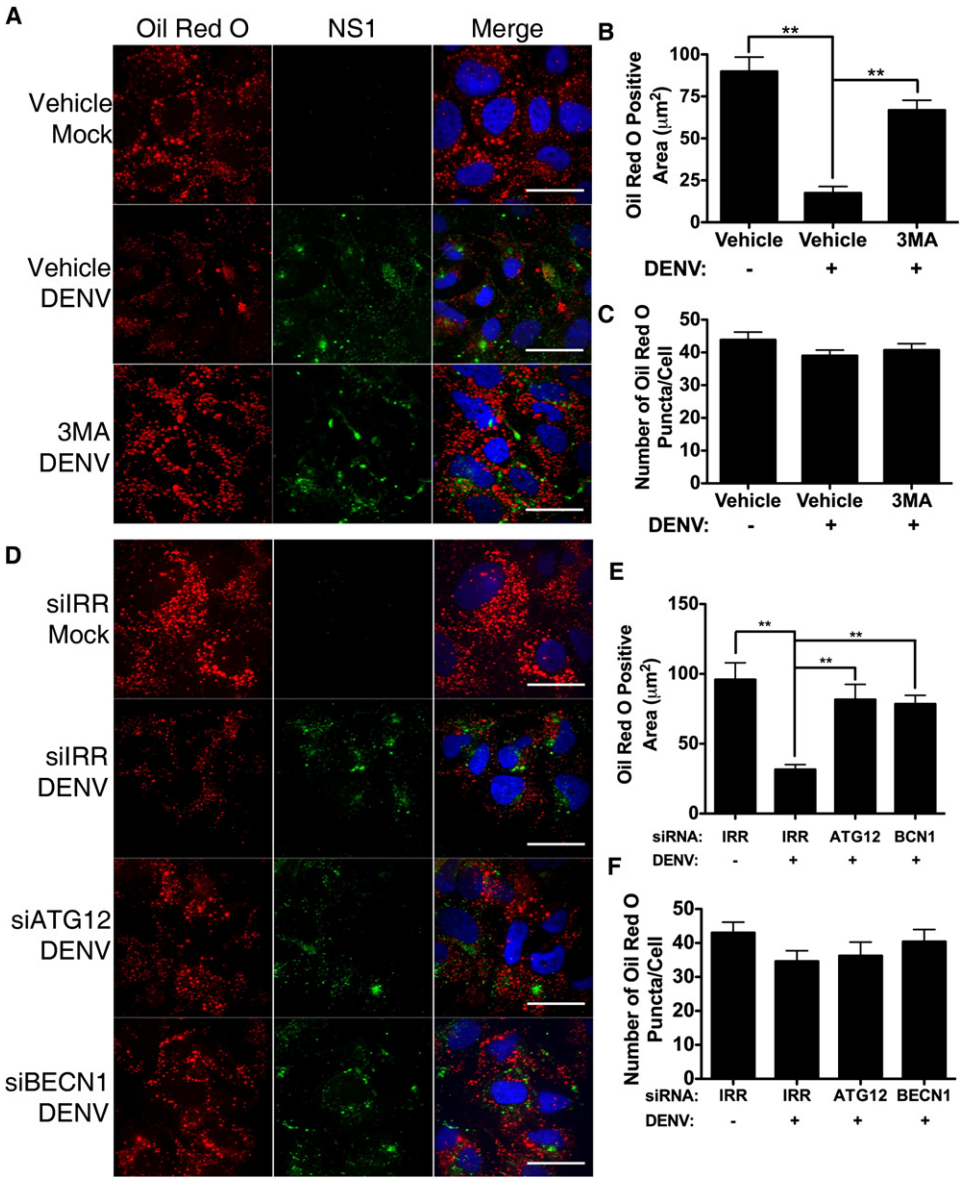

Figure 3. Inhibition of Autophagy Prevents Depletion of Lipid Droplets in DENV-Infected Cells

(A) Huh-7.5 cells were mock- or DENV-infected at an moi of 2 for 2 hr and then treated with 2.5 mM 3MA or vehicle control. Cells were fixed 48 HPI and stained with oil red O to visualize lipid droplets and an antibody against DENV NS1 (green). (D) Alternatively, Huh-7.5 cells were treated with siRNAs targeting an irrelevant HCV sequence (IRR), ATG12, or beclin1 (BECN1) for 24 hr and then infected with DENV for 48 hr at an moi of 2. ImageJ quantification of total area staining positive for oil red O (B and E) and the total number of oil red O puncta per cell (C and F) are shown. Values represent the average of at least eight cells per treatment. **$p \leq 0.001$. Scale bar represents 30 μm. Error bars represent the SEM.

GFP-LC3 puncta also stained positive for Lysotracker Red, indicative of autophagolysosomal acidification (Figures 5B and 5C). Thus, DENV does not appear to perturb autophagosomal maturation.

We next investigated whether lipids were delivered to the lysosomal compartment in an autophagy-dependent manner. DENV-infected cells expressing GFP-LC3 were analyzed for colocalization of oil red O and LC3 (Figure 4D). As previously observed, there is an association of lipid droplet markers with autophagosome markers during infection. To test whether lipids were being delivered to acidified, degradative compartments, we mock- or DENV-infected Huh-7.5 cells for 24 hr and stained them with Lysotracker and Bodipy 493/503 to label acidic compartments and lipid droplets, respectively. DENV infection increased the number of structures that were copositive for Lysotracker and the Bodipy lipid droplet marker without altering the total number of Lysotracker-positive structures (Figures 5E and 5F). Thus, DENV infection increased the delivery of lipids to acidified lysosomes. To determine the requirement of autophagy for delivery of lipids to LAMP1 compartments, we treated Huh-7.5 cells with IRR or BECN1 siRNAs and mock- or DENV-infected them for 24 hr. Cells were then fixed and probed for the association of LAMP1 with oil

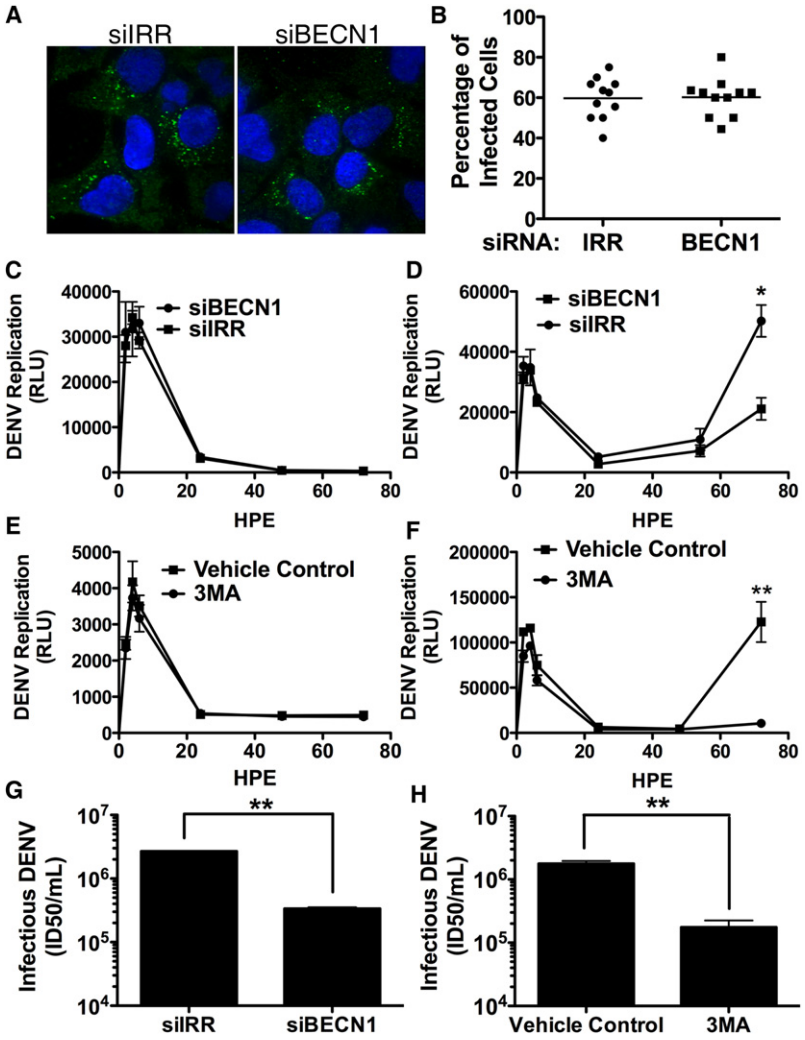

Figure 4. DENV Replication, but Not Entry or Translation, Is Dependent upon Autophagy

(A) Huh-7.5 cells silenced for BECN1 or an irrelevant control were infected (moi = 0.5) for 15 hr before fixation and staining for dsRNA and DAPI. Random fields of view were imaged (A) and quantified (B) for the percentage of cells containing DENV-specific dsRNA. A polymerase-defective DENV luciferase replicon was electroporated into Huh-7.5 cells silenced for BECN1 or treated with 3MA to measure input RNA translation (C and E, respectively). In parallel, the wild-type replicon was introduced under the same conditions to determine the effect on viral RNA replication corresponding to time points after 24 hr (D and F). Autophagy was inhibited in Huh7.5 cells via siRNAs targeting BECN1 (G) or treatment with 3MA (H), and the release of infectious DENV was quantified. *$p \leq 0.05$, **$p < 0.001$. HPE denotes hr postelectroporation. Error bars represent the SEM.

red O-stained lipids. LAMP1 structures surrounding oil red O lipids were detectable in all samples (Figure 5G). DENV infection increased the accumulation of these LAMP1/oil red O copositive structures, and this effect was significantly precluded by treatment with Beclin1 siRNAs ($p < 0.05$, Figures 5G and 5H). Thus, DENV infection enhances the delivery of lipids to the lysosome in an autophagy-dependent manner.

Triglycerides Are Specifically Depleted in DENV-Infected Cells

TGs are a major component of lipid droplets. Because lipid droplet area decreases in DENV-infected cells, we investigated whether TG levels were also reduced. Huh-7.5 cells were DENV- or mock-infected for 48 hr and total cellular lipids were extracted and separated via thin-layer chromatography (TLC). DENV infection caused a specific depletion of TGs with minimal effect on other major lipid classes. Cholesterol and cholesterol esters, which are also components of lipid droplets, are relatively unchanged by DENV infection at the whole-cell level (Figure 6A). This may reflect a selective processing of TGs; alternatively, it is possible that decreases in lipid droplet cholesterols are offset by enhanced cholesterol synthesis at sites of DENV replication, as has been proposed for West Nile virus (Mackenzie et al., 2007). We then quantified TGs in DENV-infected cells by using a colorimetric assay. DENV-infected cells had ~65% fewer TGs than mock-infected cells (Figure 6B). We also tested the requirement of autophagy for TG reduction by using 3MA and siRNAs targeting critical autophagy genes (Figures 6B and 6C). As was the case with lipid droplet degradation, inhibiting autophagy in DENV-infected cells prevented TG depletion.

β-Oxidation Is Increased by and Required for DENV Replication

During normal cellular metabolism, lipid droplet TGs are processed by lipases and released as free fatty acids (FFAs), which are transported into the mitochondria to undergo β-oxidation for ATP production. We tested whether the decrease in TGs in DENV-infected cells was associated with increased cellular β-oxidation. Huh-7.5 cells were DENV- or mock-infected for 6, 24, or 48 hr, and then ^{3}H-labeled palmitic acid was added to the cells and ^3H_2O levels (an end product of β-oxidation) were quantified. Over time, the rate of β-oxidation was significantly increased in DENV-infected cells (Figure 6D) as compared to mock-infected cells ($p < 0.001$), with kinetics similar to the lipid droplet depletion. To determine whether autophagy was contributing to the increase in cellular β-oxidation, we assayed β-oxidation in the presence of 3MA or siRNAs targeting ATG12 and BECN1 (Figures 6E and 6F). Inhibition of autophagy by 3MA significantly ($p < 0.05$) reduced the levels of β-oxidation in DENV-infected cells, although not to the level of mock-infected cells. Silencing components of the autophagy machinery inhibited the rate of β-oxidation in both mock- and DENV-infected cells, suggesting that autophagy is required for basal and virally enhanced levels of cellular β-oxidation.

We tested the dependence of DENV replication on β-oxidation with etomoxir, which inhibits β-oxidation by preventing transport

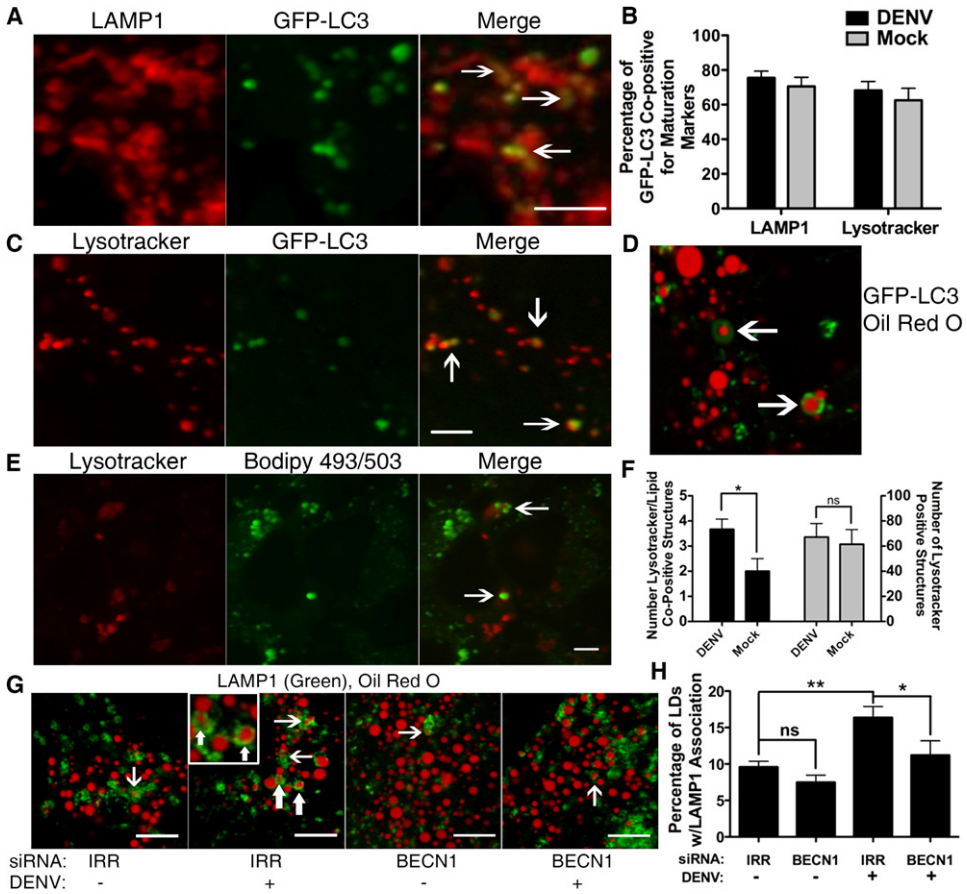

Figure 5. Increased Delivery of Lipids to Acidified Lysosomes in DENV-Infected Cells

Huh-7.5 cells were transfected with GFP-LC3, DENV-infected at an moi of 3–5 for 24 hr, and then (A) fixed and probed with antibodies against LAMP1 or (C) stained with Lysotracker. (B) ImageJ quantitation of colocalization of GFP-LC3 with LAMP1 or Lysotracker is shown. (D) GFP-LC3-transfected cells were DENV-infected for 24 hr and the association of oil red O and GFP-LC3 was visualized. (E) Huh-7.5 cells were DENV-infected (moi = 2) for 24 hr before treatment with Lysotracker and Bodipy 493/503 to stain lipid droplets. Arrows indicate examples of Lysotracker-positive structures containing lipids and are quantified in (F). The numbers of Lysotracker-positive or Lysotracker/lipid copositive structures in (F) are per field of view. (G) Huh-7.5 cells were treated with indicated siRNAs and maintained for 48 hr and then mock- or DENV-infected at an moi of 2 for 24 hr, fixed, and stained with oil red O and antibodies against LAMP1. Arrows depict examples of copositive structures. (H) ImageJ quantitation of ten randomly selected fields of view from (E) is shown. *$p < 0.05$, **$p < 0.001$. Scale bars represent 5 μm. Error bars represent the SEM.

of FFAs into the mitochondria. We first verified that etomoxir treatment significantly inhibited β-oxidation in our assay (Figure S5A). Huh-7.5 cells were then infected with DENV for 4 hr and then treated with the indicated concentrations of etomoxir to inhibit β-oxidation. Twenty-four hours, viral titer was determined by limiting dilution titer and RNA was harvested to measure viral RNA by quantitative RT-PCR. DENV RNA replication and the release of extracellular virus were inhibited in a dose-dependent manner, while no significant changes in cellular viability occurred (Figures 6G and 6H). Thus, optimal DENV replication requires robust β-oxidation. It was recently predicted that cellular enzymes involved in β-oxidation may be regulated in HCV infection, based on cellular proteomic, lipidomic, and microarray data (Blackham et al., 2010; Diamond et al., 2010). Therefore, we also examined the effects of etomoxir on HCV replication (Figure S5B). Although higher concentrations of etomoxir led to an inhibition of HCV replication, HCV does not appear to be as sensitive to the inhibition of β-oxidation as is DENV. Thus, the replication of multiple viruses may be influenced by rates of cellular β-oxidation; however, their sensitivities to this process appear to differ.

Regulation of Lipid Metabolism Is the Critical Function of Autophagy for DENV Replication

Autophagy regulates multiple cellular processes. In order to test whether its regulation of lipid metabolism was the critical function for DENV replication, we developed a lipid complementation assay. If DENV replication requires autophagosomal processing of TGs to release FFAs, then we should be able to complement defects in autophagy by adding exogenous FFAs to DENV-infected cells. DENV replication was quantified in the presence of 3MA with an exogenously added fatty acid (oleic acid) conjugated to BSA, as compared to BSA-only-treated control cells, by using the DENV luciferase reporter replicon. We first titrated the levels of BSA-oleic acid to define concentrations that did not alter DENV replication and then repeated the 3MA inhibition assay in the presence of BSA or BSA-oleic acid. In the control

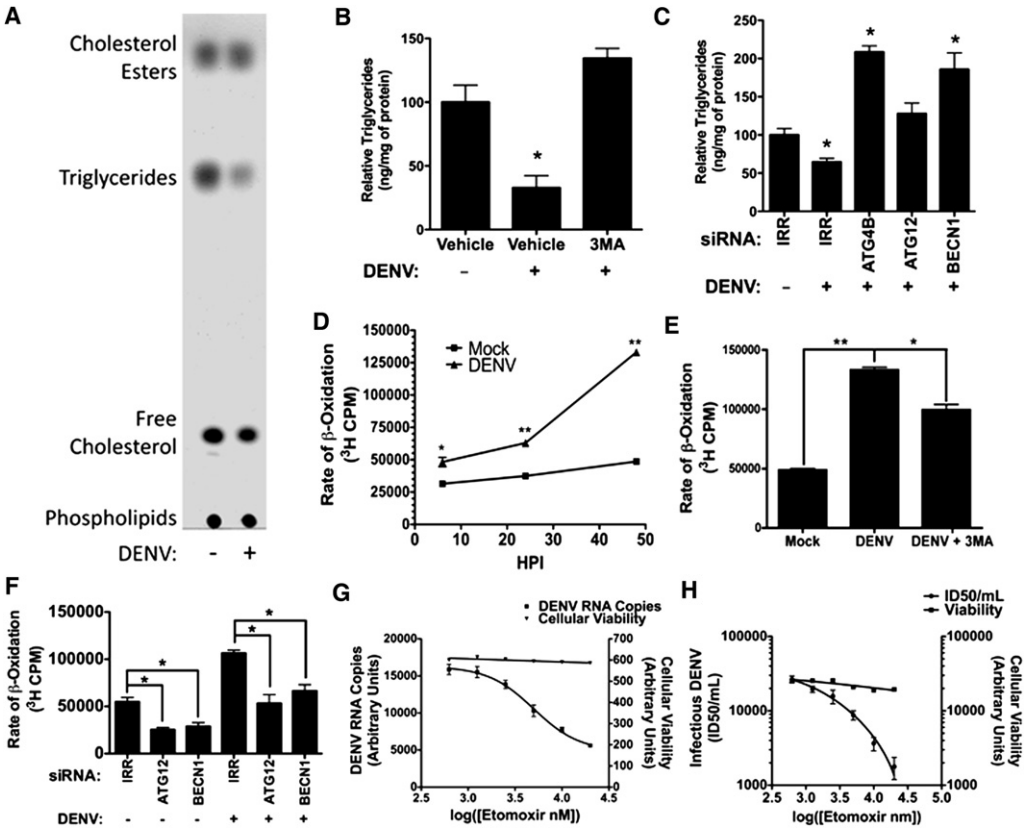

Figure 6. DENV Infection Depletes TGs and Increases β-Oxidation in an Autophagy-Dependent Manner

(A–C) DENV infection depletes TGs in an autophagy-dependent manner. (A) DENV- or mock-infected cells (moi = 2) were harvested 48 HPI and total cellular lipids were extracted. Several major lipid classes were then resolved by TLC in a nonpolar mobile phase. A representative TLC image (n = 6) is shown.

(B) Huh-7.5 cells were mock-, DENV-, or DENV+3MA-infected (moi = 2) for 48 hr. Cellular lipids were then extracted, and the amount of TGs was quantified (n = 3) relative to a protein-loading control by colorimetric assay. *$p \leq 0.05$.

(C) Huh-7.5 cells were maintained for 24 hr after introduction of irrelevant (IRR), ATG4B, ATG12, or BECN1 siRNAs and then were mock- or DENV-infected (moi = 2) for 48 hr. TGs were quantified as in (B).

(D–G) DENV infection increases and requires β-oxidation in an autophagy-dependent manner. (D) Huh-7.5 cells were DENV- or mock-infected (moi = 2) for the indicated times and then pulsed for 2 hr with ^{3}H-labeled palmitic acid to determine the rate of β-oxidation by measuring ^3H_2O (a byproduct of β-oxidation) via scintillation counting.

(E) Huh-7.5 cells were mock-, DENV-, or DENV+3MA-infected (moi = 2) for 48 hr. β-oxidation was measured as in (D).

(F) Huh-7.5 cells were transfected with the indicated siRNA (or irrelevant control) for 48 hr and then DENV-infected for 32 hr. β-oxidation was measured as in (D).

Huh-7.5 cells were DENV-infected for 4 hr and then treated with the indicated concentrations of etomoxir to inhibit β-oxidation. Twenty-four hours postinfection, (G) DENV RNA or (H) infectious DENV production was quantified. *$p \leq 0.05$, **$p \leq 0.001$. Error bars represent the SEM.

BSA-treated cells, 3MA inhibited DENV replication in a dose-dependent manner. In contrast, BSA-oleic acid-treated cells maintained wild-type levels of replication in the presence of increasing doses of 3MA (Figure 7A). The complementation assay was repeated with infectious DENV and exogenous lipids were able to complement autophagy inhibition for both DENV replication and infectious virus production (Figures 7B and 7C). Similarly, inhibiting autophagy with siRNAs leads to a decrease in viral RNA and titer, which can be complemented with the addition of exogenous fatty acid (Figures 7D and 7E). Cellular viability was unaltered in these assays (Figure S6). Thus, the requirement of autophagy for DENV replication can be supplanted by the addition of fatty acids.

Treatment with 3MA and etomoxir led to an additive inhibition of DENV replication, as is expected of drugs that inhibit different steps of the same pathway (the modulation of lipid metabolism for energy production) (Figure 7F). We next tested whether effective complementation of autophagy inhibitors with exogenous fatty acids required β-oxidation. The complementation assay was repeated in the absence and presence of etomoxir. We observed, as before, that we can complement the 3MA DENV replication defect by adding fatty acids. However, the addition of etomoxir prevents complementation of the viral RNA replication defect (Figure 7F). We conclude that the complementation of autophagy by exogenous lipids requires functional β-oxidation. Taken together, the data indicate that the primary function of autophagy in DENV replication is the regulation of lipid metabolism.

DISCUSSION

Autophagy is critical for the replication of numerous viruses. In many cases, autophagosomes have been proposed to be sites

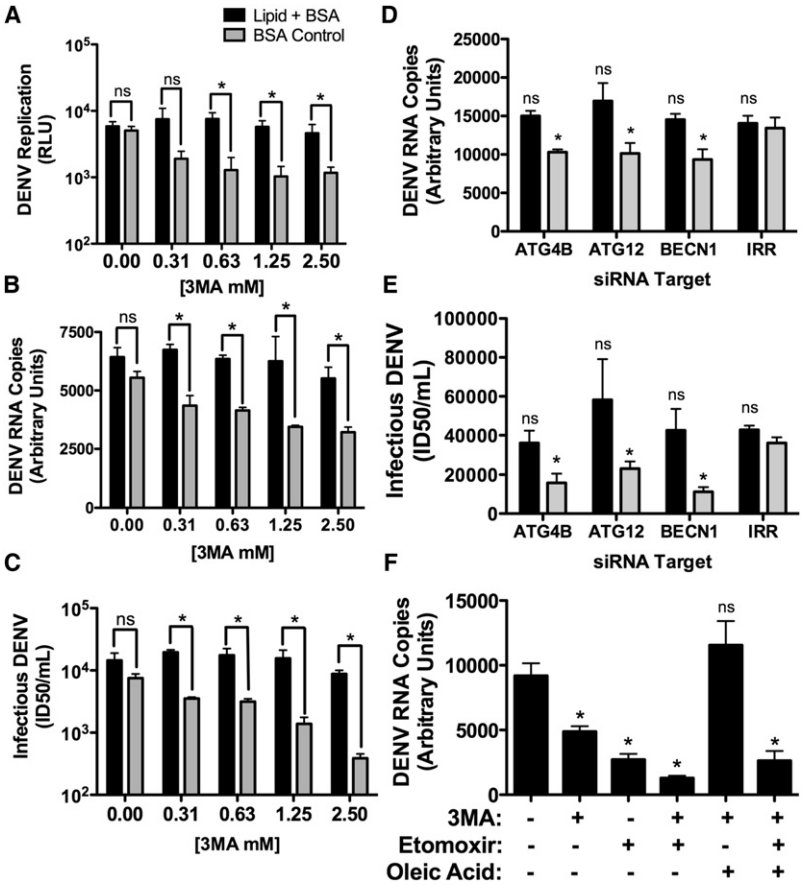

Figure 7. Defects in DENV Replication Caused by Autophagy Inhibition Can Be Complemented by Exogenous FFAs

(A) Huh-7.5 cells were electroporated with DENV luciferase reporter replicon RNAs. Twenty-four hours postelectroporation, media were replaced with 3MA supplemented with oleic acid conjugated to BSA or with BSA alone. Twenty-four hours after addition of the drug, cells were lysed and the amount of DENV replication was assayed via luciferase assay. (B and C) Huh-7.5 cells were infected for 4 hr (moi = 0.5), then virus was removed and 3MA was applied at the indicated concentrations. The media were supplemented with an oleic acid-BSA conjugate or BSA alone. Forty-eight hours postinfection, total RNA (B) or infectious DENV (C) production was quantified. (D and E) Huh-7.5 cells were treated with the indicated siRNAs, maintained for 24 hr, and mock- or DENV-infected (moi = 2) for 24 hr, and then (D) DENV RNA or (E) infectious DENV was quantified. (F) Huh-7.5 cells were infected for 4 hr (moi = 0.5) and then virus was removed and the indicated inhibitors were applied. Twenty-four hours after addition of the drug, DENV RNA was quantified. *$p \leq 0.05$. Error bars represent the SEM.

of viral RNA replication (reviewed by Wileman, 2006; Deretic and Levine, 2009). In this study, we define a different function for autophagy in viral RNA replication: the regulation of lipid metabolism. We show that DENV infection led to the processing of cellular lipid droplets and TGs. The depletion of lipid droplet area correlates with an increase in autophagosomes. DENV infection stimulates β-oxidation, which is required for DENV replication. All of these DENV-induced cellular alterations require autophagy. To confirm that fatty acid release from lipid droplets is the major role of autophagy in DENV infection, we demonstrated that the requirement of autophagy for DENV replication could be supplanted by adding exogenous fatty acids to infected cells. These data suggest a model wherein DENV infection induces autophagy, which leads to the depletion of lipid droplet TG stores. This results in the release of FFAs, which are imported into the mitochondria where they undergo β-oxidation, which generates ATP and facilitates robust viral RNA replication. Because ATP is the critical molecule for cellular energy and an important enzymatic cofactor, increased ATP levels would enhance numerous functions in DENV replication. All mammalian cell types examined thus far have the ability to generate lipid droplets (reviewed by Martin and Parton, 2006). Monocytes, which are thought to be a primary target of DENV, may have additional roles for autophagy including antigen presentation and innate immunity.

DENV has been proposed to assemble capsids at the ER in membranes directly adjacent to replication complexes, based on cryo-EM tomography studies (Welsch et al., 2009). Alternatively, lipid droplets have been suggested to be a site of DENV capsid assembly (Samsa et al., 2009). Despite the possibility that DENV may assemble at lipid droplets, it is clear that the autophagy-dependent lipid droplet modifications do not impede infectious virus assembly and release. There is a positive correlation between autophagy induction, lipid droplet depletion, robust DENV replication, and infectious virus release.

It is well established that a variety of intracellular pathogens modulate the metabolic state of the host cell. There are clear examples of both eukaryotic and bacterial pathogens that manipulate host lipid metabolism (reviewed in van der Meer-Janssen et al., 2010). *Trypanosoma cruzi* replication vacuoles are found in close proximity to, attached to, or even containing lipid droplets (Melo et al., 2006). Similarly, *Chlamydia trachomatis* recruits and internalizes lipid droplets into their resident cellular vacuoles for nutrient acquisition (Kumar et al., 2006).

Other viral infections also manipulate cellular lipid metabolism. Early work on poliovirus and Semliki Forest virus showed a requirement for phospholipid biosynthesis during viral infection (Guinea and Carrasco, 1990, 1991; Perez et al., 1991). Brome mosaic virus replication is dependent on specific localized lipid compositions (Lee and Ahlquist, 2003; Lee et al., 2001). Cytomegalovirus infection profoundly alters cellular metabolism, including increases in fatty acid synthesis, glycolysis, the citric acid cycle, and nucleotide biosynthesis (Munger et al., 2006; Munger et al., 2008). West Nile virus induces cholesterol biosynthesis and redistributes cholesterol to viral RNA replication membranes (Mackenzie et al., 2007). DENV RNA replication also requires cholesterol synthesis (Rothwell et al., 2009), and the DENV nonstructural protein 3 recruits and stimulates fatty acid synthase activity at sites of viral replication (Heaton et al.,

2010). Hepatitis B virus induces accumulation of a specific cholesterol precursor (Rodgers et al., 2009).

HCV globally alters cellular cholesterol synthesis and lipid metabolism, as shown in a recent proteomic and lipidomic study (Diamond et al., 2010). After HCV infection, there is an early increase in host catabolic and biosynthetic activities, later followed by compensatory metabolic changes. HCV alterations in lipid metabolism appear to be mediated in part by an inhibition of the AMP-activated protein kinase (Mankouri et al., 2010). In addition to alterations in lipid metabolism, HCV and some enteroviruses also depend on phospholipid signaling for replication (Berger et al., 2009; Berger and Randall, 2009; Borawski et al., 2009; Hsu et al., 2010; Li et al., 2009; Tai et al., 2009; Trotard et al., 2009; Vaillancourt et al., 2009). HIV-1 infection stimulates similar changes, with alterations in glycolysis, the tricarboxylic acid cycle, and cholesterol synthesis (Chan et al., 2007; Chan et al., 2009; Ringrose et al., 2008).

Lipids also play an important role in virion secretion and infectivity. HCV assembles virions at lipid droplets, and secretion of infectious virus is dependent upon the very low-density lipid secretion pathway (Chang et al., 2007; Huang et al., 2007). A number of viruses manipulate the lipid content of viral envelopes. HCV virions associate with lipids and apolipoproteins, and this is thought to alter the physical properties of virions, in addition to greatly enhancing infectivity (André et al., 2002, 2005). Finally, HIV-1 Nef alters cellular lipid microdomains and the lipid composition of virions (Brügger et al., 2007).

It is clear that many intracellular pathogens have a dependence on cellular lipids. Viruses appear to have this requirement at multiple stages of the viral life cycle and frequently manipulate lipid metabolism to enhance viral production. The induction of autophagy is one mechanism by which viruses can alter cellular lipid metabolism.

EXPERIMENTAL PROCEDURES

Cells, Virus, and Plasmids

Huh-7.5 cells, a subline derived from the hepatocyte Huh7 cell line (Blight et al., 2002), were primarily used in this study. In addition, the human hepatocyte cell lines Huh-7 and HepG2 and the baby hampster kidney cell line BHK were also used. Cells were maintained in DMEM-high-glucose supplemented with 0.1 mM nonessential amino acids, 5% FBS, and penicillin-streptomycin (Invitrogen). Infectious DENV-2 16681 and a DENV luciferase reporter replicon containing only the nonstructural proteins (Heaton et al., 2010) were used. GFP-LC3 was constructed by PCR amplification of LC3 from a cDNA clone (Open Biosystems), which was cloned into a C-terminal monomeric GFP fusion vector, generously provided by Benjamin Glick (The University of Chicago).

Pharmacological Inhibitor Studies

3-Methyladenine (MP Biomedicals), etomoxir (US Biological), and BSA-oleic acid (Sigma) were used. Huh-7.5 cells were infected at an moi of 0.5 for 4 hr, the inoculum was removed, and fresh media containing the inhibitor or vehicle alone were added to the cells and maintained for indicated times. Virus in cellular supernatants was quantified by titration, while intracellular RNA was isolated at 24 or 48 HPI with an RNeasy kit (QIAGEN) and quantified by real time RT-PCR, as previously described (Heaton et al., 2010; see Supplemental Experimental Procedures). For lipid complementation assays, 3MA or siRNAs were applied as described above with the addition of a 1:100 dilution of BSA-oleic acid (Sigma) or the equivalent concentration of BSA alone. For DENV-replicon assays, cells were treated with 3MA ± lipid or BSA control 24 hr after electroporation. Twenty-four hours after drug addition, DENV replication was determined via use of the Renilla Luciferase Assay System per the manufacturer's instruction (Promega). For the combination drug studies, cells were infected at an moi of 0.5 for 4 hr, and then the inoculum was replaced with 2.5 mM 3MA, 20 μM etomoxir, or a combination of the two. BSA-lipid was used at a 1:100 dilution as before. RNA was quantified ~24 HPI. Cell viability was assayed with an MTT or CellTiter-Glo assay kit (Promega).

Immunofluorescence

Cells were infected at an moi of 1–5 for 24–48 hr in DMEM supplemented with either 1% or 5% FBS before methanol or paraformaldehyde plus saponin fixation and antibody staining. Antibodies used included dsRNA (English and Scientific Consulting Bt.), NS1 (Abcam), LAMP1 (Abcam), NS3 (gift of Richard Kuhn, Purdue University), the DENV2-specific monoclonal antibody D1-4G2-4-15 (ATCC), and Alexa-fluor 488 or 594 secondary antibodies (Invitrogen). Stained coverslips were mounted with Prolong Gold with DAPI (Invitrogen). Oil red O (MP Biomedicals) was used per the manufacturer's instructions. Lysotracker (50 nM) and 20 μg/ml Bodipy 20 493/503 (Invitrogen) were visualized in live cells. Images were acquired with an Olympus DSU confocal microscope with a 100× oil objective or with a Leica SP5 tandem scanner, two-photon spectral confocal system with a 100× oil objective with digital zoom. Digital images were taken with Slidebook 4.1 software and processed with ImageJ (National Institutes of Health) and Adobe Photoshop. Quantification of images was performed with ImageJ and a set of defined intensity thresholds that were applied to all images.

Electron Microscopy

Huh-7.5 cells were maintained in 1% DMEM, DENV infected (moi = 5) for 48 HPI and processed for EM by standard procedures (see Supplemental Experimental Procedures). Images were taken at 300 kV with an FEI Tecnai F30 electron microscope equipped with a high-performance Gatan CCD camera. The average diameters of the observed lipid droplets were calculated by averaging multiple diameter measurements with ImageJ software. The volume of the lipid droplets was calculated by using the average diameter in the equation $v = 4/3\pi r^3$.

siRNA Inhibition

siRNAs were introduced into cells by using RNAiMax (Invitrogen) according to the manufacturer's instructions for optimal periods, depending on gene. The siRNA sequences and the Taqman assays used to verify knockdown relative to 18S control are described in Table S1.

Cellular Lipid Analysis

Huh-7.5 cells in 2% DMEM were DENV- or mock-infected at an moi of 2 for 48 hr, washed in PBS, then scraped, pelleted, and resuspended in a glass tube in 400 μl of methanol:chloroform (1:2 v/v). Lipids were extracted via the Folch procedure (Folch et al., 1957) and processed by standard TLC, as described in Supplemental Experimental Procedures.

β-Oxidation Assay

Huh-7.5 cells were infected at an moi of 3 in 2% FBS DMEM. Unlabeled palmitic acid (10 mM) and ^{3}H-labeled palmitic acid (10 μCi/ml) were conjugated to 7.5 μM of fatty acid-free BSA (1:450 dilution). At the indicated time point, the DMEM was replaced with 500 μl of the palmitic acid-BSA mixture in Kreb's buffer (5 μCi/6 wells) and incubated at 37°C for 2 hr. The Kreb's buffer was removed from the cells and added to an equal volume of 10% trichloroacetic acid. After incubation at RT for 5 min, solution was spun at 13,000 × g for 5 min, 500 μl of the supernatant was removed and added to 100 μl 6N NaOH, mixed, and then applied to 90 μm pore columns (Spectrum Labs) that were packed with a Dowex 1 × 8 100–200 mesh ion exchange resin (Acros Organics). The ^3H_2O was eluted with 1 ml ddH_20 and assayed for ^{3}H with a scintillation counter.

Statistical Analysis

All statistical significance was determined by using either a paired or an unpaired Student's t test depending on the experimental design. Statistical analysis of microscopy images was based on ImageJ quantification of randomly selected fields of view or cells ($n > 5$) for each treatment or time point.

Each study shown is representative of at least two independent experiments. The level of significance is denoted in each figure (*$p \leq 0.05$, **$p \leq 0.001$).

SUPPLEMENTAL INFORMATION

Supplemental Information includes six figures, one table, and Supplemental Experimental Procedures and can be found with this article online at doi:10.1016/j.chom.2010.10.006.

ACKNOWLEDGMENTS

We thank Benjamin Glick (University of Chicago) for providing pmGFP-C1, Charles Rice (Rockefeller University) for providing Huh-7.5 cells, Rushika Perera and Richard Kuhn (Purdue University) for providing the DENV replicon and NS3 antibody, and Claire Huang (CDC, Fort Collins CO) for providing the DENV-2 16681 infectious clone. We thank Ernst Lengyel, Songul Dogan, and Kristin Nieman for technical expertise with the β-oxidation studies. We thank Kristi Berger, Rushika Perera, and Richard Kuhn for critical reading of the manuscript. The authors wish to acknowledge membership within and support from the Region V Great Lakes RCE (NIH award 1-U54-AI-057153). N.S.H. is funded by NIH training grant T32 AI065382-01.

Received: March 16, 2010
Revised: June 29, 2010
Accepted: October 11, 2010
Published: November 17, 2010

REFERENCES

André, P., Komurian-Pradel, F., Deforges, S., Perret, M., Berland, J.L., Sodoyer, M., Pol, S., Bréchot, C., Paranhos-Baccalà, G., and Lotteau, V. (2002). Characterization of low- and very-low-density hepatitis C virus RNA-containing particles. J. Virol. *76*, 6919–6928.

André, P., Perlemuter, G., Budkowska, A., Bréchot, C., and Lotteau, V. (2005). Hepatitis C virus particles and lipoprotein metabolism. Semin. Liver Dis. *25*, 93–104.

Berger, K.L., and Randall, G. (2009). Potential roles for cellular cofactors in hepatitis C virus replication complex formation. Commun. Integr. Biol. *2*, 471–473.

Berger, K.L., Cooper, J.D., Heaton, N.S., Yoon, R., Oakland, T.E., Jordan, T.X., Mateu, G., Grakoui, A., and Randall, G. (2009). Roles for endocytic trafficking and phosphatidylinositol 4-kinase III alpha in hepatitis C virus replication. Proc. Natl. Acad. Sci. USA *106*, 7577–7582.

Blackham, S., Baillie, A., Al-Hababi, F., Remlinger, K., You, S., Hamatake, R., and McGarvey, M.J. (2010). Gene expression profiling indicates the roles of host oxidative stress, apoptosis, lipid metabolism, and intracellular transport genes in the replication of hepatitis C virus. J. Virol. *84*, 5404–5414.

Blight, K.J., McKeating, J.A., and Rice, C.M. (2002). Highly permissive cell lines for subgenomic and genomic hepatitis C virus RNA replication. J. Virol. *76*, 13001–13014.

Borawski, J., Troke, P., Puyang, X., Gibaja, V., Zhao, S., Mickanin, C., Leighton-Davies, J., Wilson, C.J., Myer, V., Cornellataracido, I., et al. (2009). Class III phosphatidylinositol 4-kinase alpha and beta are novel host factor regulators of hepatitis C virus replication. J. Virol. *83*, 10058–10074.

Brügger, B., Krautkrämer, E., Tibroni, N., Munte, C.E., Rauch, S., Leibrecht, I., Glass, B., Breuer, S., Geyer, M., Kräusslich, H.G., et al. (2007). Human immunodeficiency virus type 1 Nef protein modulates the lipid composition of virions and host cell membrane microdomains. Retrovirology *4*, 70.

Chan, E.Y., Qian, W.J., Diamond, D.L., Liu, T., Gritsenko, M.A., Monroe, M.E., Camp, D.G., 2nd, Smith, R.D., and Katze, M.G. (2007). Quantitative analysis of human immunodeficiency virus type 1-infected CD4+ cell proteome: dysregulated cell cycle progression and nuclear transport coincide with robust virus production. J. Virol. *81*, 7571–7583.

Chan, E.Y., Sutton, J.N., Jacobs, J.M., Bondarenko, A., Smith, R.D., and Katze, M.G. (2009). Dynamic host energetics and cytoskeletal proteomes in human immunodeficiency virus type 1-infected human primary CD4 cells: analysis by multiplexed label-free mass spectrometry. J. Virol. *83*, 9283–9295.

Chang, K.S., Jiang, J., Cai, Z., and Luo, G. (2007). Human apolipoprotein e is required for infectivity and production of hepatitis C virus in cell culture. J. Virol. *81*, 13783–13793.

Deretic, V. (2005). Autophagy in innate and adaptive immunity. Trends Immunol. *26*, 523–528.

Deretic, V., and Levine, B. (2009). Autophagy, immunity, and microbial adaptations. Cell Host Microbe *5*, 527–549.

Diamond, D.L., Syder, A.J., Jacobs, J.M., Sorensen, C.M., Walters, K.A., Proll, S.C., McDermott, J.E., Gritsenko, M.A., Zhang, Q., Zhao, R., et al. (2010). Temporal proteome and lipidome profiles reveal hepatitis C virus-associated reprogramming of hepatocellular metabolism and bioenergetics. PLoS Pathog. *6*, e1000719.

Dreux, M., Gastaminza, P., Wieland, S.F., and Chisari, F.V. (2009). The autophagy machinery is required to initiate hepatitis C virus replication. Proc. Natl. Acad. Sci. USA *106*, 14046–14051.

Folch, J., Lees, M., and Sloane Stanley, G.H. (1957). A simple method for the isolation and purification of total lipides from animal tissues. J. Biol. Chem. *226*, 497–509.

Guinea, R., and Carrasco, L. (1990). Phospholipid biosynthesis and poliovirus genome replication, two coupled phenomena. EMBO J. *9*, 2011–2016.

Guinea, R., and Carrasco, L. (1991). Effects of fatty acids on lipid synthesis and viral RNA replication in poliovirus-infected cells. Virology *185*, 473–476.

Haemmerle, G., Zimmermann, R., and Zechner, R. (2003). Letting lipids go: hormone-sensitive lipase. Curr. Opin. Lipidol. *14*, 289–297.

Heaton, N.S., Perera, R., Berger, K.L., Khadka, S., Lacount, D.J., Kuhn, R.J., and Randall, G. (2010). Dengue virus nonstructural protein 3 redistributes fatty acid synthase to sites of viral replication and increases cellular fatty acid synthesis. Proc. Natl. Acad. Sci. USA *107*, 17345–17350.

Hsu, N.Y., Ilnytska, O., Belov, G., Santiana, M., Chen, Y.H., Takvorian, P.M., Pau, C., van der Schaar, H., Kaushik-Basu, N., Balla, T., et al. (2010). Viral reorganization of the secretory pathway generates distinct organelles for RNA replication. Cell *141*, 799–811.

Huang, H., Sun, F., Owen, D.M., Li, W., Chen, Y., Gale, M., Jr., and Ye, J. (2007). Hepatitis C virus production by human hepatocytes dependent on assembly and secretion of very low-density lipoproteins. Proc. Natl. Acad. Sci. USA *104*, 5848–5853.

Jackson, W.T., Giddings, T.H., Jr., Taylor, M.P., Mulinyawe, S., Rabinovitch, M., Kopito, R.R., and Kirkegaard, K. (2005). Subversion of cellular autophagosomal machinery by RNA viruses. PLoS Biol. *3*, e156.

Jormakka, M., Byrne, B., and Iwata, S. (2003). Protonmotive force generation by a redox loop mechanism. FEBS Lett. *545*, 25–30.

Khakpoor, A., Panyasrivanit, M., Wikan, N., and Smith, D.R. (2009). A role for autophagolysosomes in dengue virus 3 production in HepG2 cells. J. Gen. Virol. *90*, 1093–1103.

Kirkegaard, K., Taylor, M.P., and Jackson, W.T. (2004). Cellular autophagy: surrender, avoidance and subversion by microorganisms. Nat. Rev. Microbiol. *2*, 301–314.

Komatsu, M., Waguri, S., Ueno, T., Iwata, J., Murata, S., Tanida, I., Ezaki, J., Mizushima, N., Ohsumi, Y., Uchiyama, Y., et al. (2005). Impairment of starvation-induced and constitutive autophagy in Atg7-deficient mice. J. Cell Biol. *169*, 425–434.

Kumar, Y., Cocchiaro, J., and Valdivia, R.H. (2006). The obligate intracellular pathogen Chlamydia trachomatis targets host lipid droplets. Curr. Biol. *16*, 1646–1651.

Lee, W.M., and Ahlquist, P. (2003). Membrane synthesis, specific lipid requirements, and localized lipid composition changes associated with a positive-strand RNA virus RNA replication protein. J. Virol. *77*, 12819–12828.

Lee, W.M., Ishikawa, M., and Ahlquist, P. (2001). Mutation of host delta9 fatty acid desaturase inhibits brome mosaic virus RNA replication between template recognition and RNA synthesis. J. Virol. *75*, 2097–2106.

Lee, Y.R., Lei, H.Y., Liu, M.T., Wang, J.R., Chen, S.H., Jiang-Shieh, Y.F., Lin, Y.S., Yeh, T.M., Liu, C.C., and Liu, H.S. (2008). Autophagic machinery activated by dengue virus enhances virus replication. Virology *374*, 240–248.

Li, Q., Brass, A.L., Ng, A., Hu, Z., Xavier, R.J., Liang, T.J., and Elledge, S.J. (2009). A genome-wide genetic screen for host factors required for hepatitis C virus propagation. Proc. Natl. Acad. Sci. USA *106*, 16410–16415.

Liang, X.H., Kleeman, L.K., Jiang, H.H., Gordon, G., Goldman, J.E., Berry, G., Herman, B., and Levine, B. (1998). Protection against fatal Sindbis virus encephalitis by beclin, a novel Bcl-2-interacting protein. J. Virol. *72*, 8586–8596.

Mackenzie, J.M., Khromykh, A.A., and Parton, R.G. (2007). Cholesterol manipulation by West Nile virus perturbs the cellular immune response. Cell Host Microbe *2*, 229–239.

Mankouri, J., Tedbury, P.R., Gretton, S., Hughes, M.E., Griffin, S.D., Dallas, M.L., Green, K.A., Hardie, D.G., Peers, C., and Harris, M. (2010). Enhanced hepatitis C virus genome replication and lipid accumulation mediated by inhibition of AMP-activated protein kinase. Proc. Natl. Acad. Sci. USA *107*, 11549–11554.

Martin, S., and Parton, R.G. (2006). Lipid droplets: a unified view of a dynamic organelle. Nat. Rev. Mol. Cell Biol. *7*, 373–378.

McGarry, J.D., and Brown, N.F. (1997). The mitochondrial carnitine palmitoyltransferase system. From concept to molecular analysis. Eur. J. Biochem. *244*, 1–14.

Melo, R.C., Fabrino, D.L., Dias, F.F., and Parreira, G.G. (2006). Lipid bodies: structural markers of inflammatory macrophages in innate immunity. Inflamm. Res. *55*, 342–348.

Miller, S., and Krijnse-Locker, J. (2008). Modification of intracellular membrane structures for virus replication. Nat. Rev. Microbiol. *6*, 363–374.

Miller, S., Kastner, S., Krijnse-Locker, J., Bühler, S., and Bartenschlager, R. (2007). The non-structural protein 4A of dengue virus is an integral membrane protein inducing membrane alterations in a 2K-regulated manner. J. Biol. Chem. *282*, 8873–8882.

Mizushima, N. (2007). Autophagy: process and function. Genes Dev. *21*, 2861–2873.

Mizushima, N., Ohsumi, Y., and Yoshimori, T. (2002). Autophagosome formation in mammalian cells. Cell Struct. Funct. *27*, 421–429.

Munger, J., Bajad, S.U., Coller, H.A., Shenk, T., and Rabinowitz, J.D. (2006). Dynamics of the cellular metabolome during human cytomegalovirus infection. PLoS Pathog. *2*, e132.

Munger, J., Bennett, B.D., Parikh, A., Feng, X.J., McArdle, J., Rabitz, H.A., Shenk, T., and Rabinowitz, J.D. (2008). Systems-level metabolic flux profiling identifies fatty acid synthesis as a target for antiviral therapy. Nat. Biotechnol. *26*, 1179–1186.

Orvedahl, A., Alexander, D., Tallóczy, Z., Sun, Q., Wei, Y., Zhang, W., Burns, D., Leib, D.A., and Levine, B. (2007). HSV-1 ICP34.5 confers neurovirulence by targeting the Beclin 1 autophagy protein. Cell Host Microbe *1*, 23–35.

Panyasrivanit, M., Khakpoor, A., Wikan, N., and Smith, D.R. (2009). Co-localization of constituents of the dengue virus translation and replication machinery with amphisomes. J. Gen. Virol. *90*, 448–456.

Perez, L., Guinea, R., and Carrasco, L. (1991). Synthesis of Semliki Forest virus RNA requires continuous lipid synthesis. Virology *183*, 74–82.

Perlmutter, D.H. (2002). Liver injury in alpha1-antitrypsin deficiency: an aggregated protein induces mitochondrial injury. J. Clin. Invest. *110*, 1579–1583.

Ren, Y., and Schulz, H. (2003). Metabolic functions of the two pathways of oleate beta-oxidation double bond metabolism during the beta-oxidation of oleic acid in rat heart mitochondria. J. Biol. Chem. *278*, 111–116.

Ringrose, J.H., Jeeninga, R.E., Berkhout, B., and Speijer, D. (2008). Proteomic studies reveal coordinated changes in T-cell expression patterns upon infection with human immunodeficiency virus type 1. J. Virol. *82*, 4320–4330.

Rodgers, M.A., Saghatelian, A., and Yang, P.L. (2009). Identification of an overabundant cholesterol precursor in hepatitis B virus replicating cells by untargeted lipid metabolite profiling. J. Am. Chem. Soc. *131*, 5030–5031.

Rothwell, C., Lebreton, A., Young Ng, C., Lim, J.Y., Liu, W., Vasudevan, S., Labow, M., Gu, F., and Gaither, L.A. (2009). Cholesterol biosynthesis modulation regulates dengue viral replication. Virology *389*, 8–19.

Samsa, M.M., Mondotte, J.A., Iglesias, N.G., Assunção-Miranda, I., Barbosa-Lima, G., Da Poian, A.T., Bozza, P.T., and Gamarnik, A.V. (2009). Dengue virus capsid protein usurps lipid droplets for viral particle formation. PLoS Pathog. *5*, e1000632.

Schmid, D., Dengjel, J., Schoor, O., Stevanovic, S., and Münz, C. (2006). Autophagy in innate and adaptive immunity against intracellular pathogens. J. Mol. Med. *84*, 194–202.

Shelly, S., Lukinova, N., Bambina, S., Berman, A., and Cherry, S. (2009). Autophagy is an essential component of Drosophila immunity against vesicular stomatitis virus. Immunity *30*, 588–598.

Singh, R., Kaushik, S., Wang, Y., Xiang, Y., Novak, I., Komatsu, M., Tanaka, K., Cuervo, A.M., and Czaja, M.J. (2009). Autophagy regulates lipid metabolism. Nature *458*, 1131–1135.

Sir, D., Chen, W.L., Choi, J., Wakita, T., Yen, T.S., and Ou, J.H. (2008). Induction of incomplete autophagic response by hepatitis C virus via the unfolded protein response. Hepatology *48*, 1054–1061.

Tai, A.W., Benita, Y., Peng, L.F., Kim, S.S., Sakamoto, N., Xavier, R.J., and Chung, R.T. (2009). A functional genomic screen identifies cellular cofactors of hepatitis C virus replication. Cell Host Microbe *5*, 298–307.

Taylor, M.P., and Kirkegaard, K. (2007). Modification of cellular autophagy protein LC3 by poliovirus. J. Virol. *81*, 12543–12553.

Trotard, M., Lepère-Douard, C., Régeard, M., Piquet-Pellorce, C., Lavillette, D., Cosset, F.L., Gripon, P., and Le Seyec, J. (2009). Kinases required in hepatitis C virus entry and replication highlighted by small interference RNA screening. FASEB J. *23*, 3780–3789.

Tsukada, M., and Ohsumi, Y. (1993). Isolation and characterization of autophagy-defective mutants of Saccharomyces cerevisiae. FEBS Lett. *333*, 169–174.

Vaillancourt, F.H., Pilote, L., Cartier, M., Lippens, J., Liuzzi, M., Bethell, R.C., Cordingley, M.G., and Kukolj, G. (2009). Identification of a lipid kinase as a host factor involved in hepatitis C virus RNA replication. Virology *387*, 5–10.

van der Meer-Janssen, Y.P., van Galen, J., Batenburg, J.J., and Helms, J.B. (2010). Lipids in host-pathogen interactions: pathogens exploit the complexity of the host cell lipidome. Prog. Lipid Res. *49*, 1–26.

Welsch, S., Miller, S., Romero-Brey, I., Merz, A., Bleck, C.K., Walther, P., Fuller, S.D., Antony, C., Krijnse-Locker, J., and Bartenschlager, R. (2009). Composition and three-dimensional architecture of the dengue virus replication and assembly sites. Cell Host Microbe *5*, 365–375.

Wileman, T. (2006). Aggresomes and autophagy generate sites for virus replication. Science *312*, 875–878.

Wong, J., Zhang, J., Si, X., Gao, G., Mao, I., McManus, B.M., and Luo, H. (2008). Autophagosome supports coxsackievirus B3 replication in host cells. J. Virol. *82*, 9143–9153.

Yoon, S.Y., Ha, Y.E., Choi, J.E., Ahn, J., Lee, H., Kweon, H.S., Lee, J.Y., and Kim, D.H. (2008). Coxsackievirus B4 uses autophagy for replication after calpain activation in rat primary neurons. J. Virol. *82*, 11976–11978.